Study of the structural, morphological and electric characteristics of TiO$_2$ nano-powders.

M. P. F. Graça[*], C. C. Silva, L. C. Costa, M. A. Valente

Physics Department (I3N) – University of Aveiro, Campus Universitário de Santiago, 3810 – 193 – Portugal.

Abstract

Titania (TiO$_2$) has been widely studied because of its unique optical and chemical properties in catalysis, photocatalysis and nonlinear optics. This material crystallizes mainly in anatase or rutile phase and exhibits different physical and chemical properties. It is well-known that the anatase phase is suitable for catalysts and supports, while the rutile phase is used for optical and electronic purposes due to its high dielectric constant and high refractive index
Several methods of chemical synthesis have been developed and used to prepare thin films. Amongst the alternative methods, the Pechini method has been used successfully for the preparation of several types of materials. In this work, nanopowders of titanium oxide were prepared through the heat-treatment of metallic polymeric resin prepared by the polymeric precursor method (Pechini method). The resin was characterized by differential scanning calorimetry (DSC) and the powders by, X-ray diffraction (DRX) and scanning electron microscopy (SEM). Dielectric measurements were performed in function of the frequency at room temperature.

Keywords: Nanopowder, Characterization, Structural and morphological properties, Dielectric properties.
PACS: 81.07.Wx, 81.07.-b, 68.55.-a, 81.40.Tv .

---

[*]) For correspondence; Email: mpfg@ua.pt.

1. Introduction

Titanium dioxide (TiO_2) nanocrystals, are non toxic and chemically very stable, have attracted much attention due to their potential applications in humidity and oxygen sensitivity, catalysis, solar energy conversion and hydrogen gas generation. Is also used has pigment for white paints (n=2.3), for corrosion protection, in air purification system and in dielectric system requiring high dielectric constant and high resistivity [1–3].

The TiO_2 is a polymorph, existing in three different crystal phases being the most usual: anatase (tetragonal with crystals typically acute dipyramidal, but often highly modified), rutile (tetragonal and crystals prismatic, elongated and striated) and brookite (orthorhombic and non-stable) [4]. At room temperature, TiO_2 presents a gap energy of Eg= 3.0 eV and Eg= 3.2 eV if the crystal is in the rutile or anatase phase, respectively [5]. Thus, the different structures of the two phases exhibit different physical properties, leading to different applications [6].

The preparation, by the traditional routes, of the rutile phase normally requires temperatures above 1000 ºC [7]. The anatase phase is usually formed at lower temperatures. Actually, the study of the TiO_2 improved properties in function of the unusual structure are been presented namely, the anatase-rutile phase transition and the phonon nature of TiO_2 nanocrystals by Raman scattering [8]. The experimental results show that the lattice vibrational properties of TiO_2 nanocrystals have remarkable variations with respect to the bulk single-crystal. It has been showed that the TiO_2 properties can be improved if it presents a high surface area. Actually, the packaging technology demands materials having high dielectric constant and low loss tangent with improved thermal properties for the integration of passive components into a single module. High dielectric constant is needed for circuit miniaturization and low loss tangent keeps the signal integrity [9]. It is well known that the rutile phase presents high dielectric constant (>150 at room temperature) and low dielectric loss (<0.001) [6;10].

Several methods have been used for the preparation of TiO_2 powders, such as the Sol-Gel, Micelle and Inverse Micelle, Hydrothermal, Solvothermal, Direct Oxidation, Chemical Vapor Deposition, Physical Vapor Deposition, Electrodeposition, Sonochemical and Microwave Method [11]. In this work, the

preparation by the Pechini method, of nano-powders of TiO_2 with anatase, rutile and both crystal phases was achieved. The crystal structure of the samples calcinated at temperatures between 350 ºC and 800 ºC was analyzed by XRD. The morphology was investigated using SEM microscopy and the dielectric properties were investigated, at room temperature, in function of the frequency.

2. Experimental procedure

The starting materials used for the preparation of the polymeric precursor solution, by the Pechini process [12], were citric acid ($C_6H_8O_7.H_2O$), ethylene glycol ($C_2H_6O_2$), deionised water (H_2O) and titanium isopropoxide ($Ti(OCH(CH_3)_2)_4$). The first step was the formation of a transparent aqueous solution of citric acid (CA). To this solution, titanium isopropoxide was added, using the molar ratio between CA: metal cation of 1:3. The metallic citrate solution was stired magnetically and ethylene glycol (EG) was added, leading to the formation of organic ester. This solution was allowed to mix, at 70ºC, for 1 hour, promoting the polymerization process. In this experience, the CA/EG mass ratio was fixed in 2:3. The obtained resin, transparent, colourless and with some viscosity, was maintained at room temperature in a low-humidity controlled vessel.

The resin was heat-treated in air, with a heating rate of 75 ºC/h, at 350, 380, 400, 500, 600 and 800 ºC for 4 hours. These temperatures were chosen in agreement with the differential scanning calometry results (DSC), carried out with a Shimatzu DSC-50 apparatus, starting at room temperature until 500 ºC, with an heating rate of 10 ºC/min (Fig. 1).
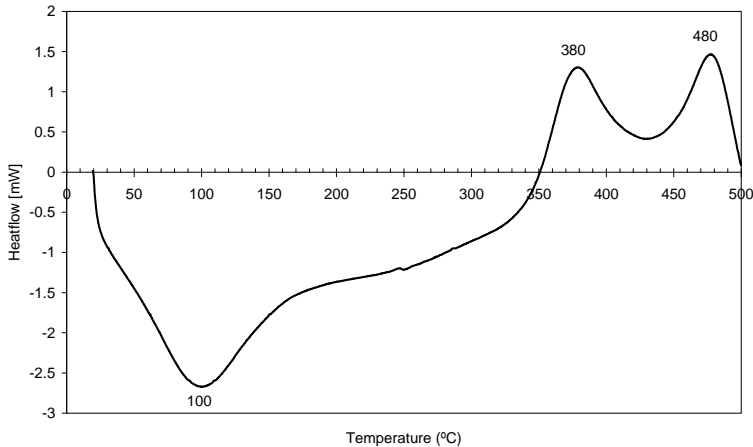
Fig. 1: DSC of the TiO$_2$ pre-treated at 300 ºC

The X-ray diffraction (XRD) patterns data were obtained on an X'Pert MPD Philips difractometer (CuKα radiation, λ=1.54056 Å) at 40 kV, and 30 mA, with a curved graphite monochromator, an automatic divergence slit (irradiated length 20.00 mm), a progressive receiving slit (height 0.05 mm) and a flat plane sample holder in a Bragg-Brentano parafocusing optics configuration. Intensity data were collected by the step counting method (step 0.02 º in 1 s) in the 2θ angle range of 10-60 º. The analyses of the crystallite size (L$_c$) of the anatase and rutile phases were done using the Scherrer's equation ($L_c = k\lambda/(\beta \cos\theta)$), where λ=0.154056nm, the wavelength of CuKα radiation, k is the shape correction factor (0.9), θ is the Bragg angle diffraction with wavelength λ and β has been recorded after taking into account of instrumental broadening. We have used LaB6 standard powder (SRM 660-National Institute of Standard Technology) to determine the instrumental width [13].

The morphology studies of the calcinated powders were observed by scanning electron microscopy (SEM) on a Hitachi S4100-1. The powders were covered with carbon before microscopic observation.

For the electrical measurements, pellets of the calcinated powders, made using a uniaxial pressure system, with 0.5 mm of thickness and 0.7 mm in diameter. The impedance spectroscopy measurements were carried out at room temperature, in the frequency range of 100 Hz - 100 kHz using a *SR850 DSP Lock-In Amplifier*, in the typical lock-in configuration, measuring the "in-phase" and "out-

of-phase" components of the output signal [14]. For these measurements the electric contacts were mechanical, i.e., the pellets were pressurized between two steel plates. No sputtered or painted electrodes were used due to the porosity – in this work no sintering process was made. The analytical background, used in the dielectric data analysis, was as follows: - The complex permittivity, $\varepsilon^* = \varepsilon' + j\varepsilon''$, was interpreted using the complex impedance formalism, $Z^* = 1/(\mu\varepsilon^*)$ [15;16] (where $\mu = j\omega C_0$, ω is the angular frequency, C_0 the admittance of the empty cell and $j = \sqrt{-1}$ [17]). The real and imaginary parts of the impedance were calculated using equation below.

$$Z^* = \frac{R_i\left(V_f V_0 - V_f^2 - V_q^2\right) - \omega C_i^2 R_i^2 V_q V_0}{\left(1 + \omega^2 C_i^2 R_i^2\right)\left(V_f^2 + V_q^2\right)} - j\,\frac{V_q V_0 R_i + \omega C_i^2 R_i^2\left(V_f V_0 - V_f^2 - V_q^2\right)}{\left(1 + \omega^2 C_i^2 R_i^2\right)\left(V_f^2 + V_q^2\right)}$$

This expression was obtained when the sample impedance is in series with a known resistance (1 KΩ) This resistance is in parallel with the lock-in input impedance. R_i is the equivalent resistance of the lock-in input resistance (100 MΩ) and the known resistance (1 KΩ C_i is the lock-in input capacitance (15 pF), V_0 is the input signal (|V_0|=1 V), and V_f and V_q the "in-phase" and "out-of-phase" components of the measured signal.

The complex modulus formalism ($M^* = 1/\varepsilon^*$), proposed by Macedo [18], was adopted to determine the relaxation time (τ_σ), because it minimizes the electrode interface capacitance contribution and others interfacial effects [17;18]. The representation of M″ versus frequency (in logarithmic scale) often shows peak(s) associated with the contribution(s) of small capacitance(s) [18;19]. The relaxation time is defined by $\tau_\sigma = (\omega_{peak})^{-1}$ where (ω_{peak}) represents the angular frequency of the M″ peak(s) [15;20].

3. Results and Discussion

The thermal analysis of the resin is presented in figures 1 and 2. In the DSC spectra (Fig.1) it can be observed the existence of three

thermodynamic phenomena, the first at approximately 100 ºC, can be attributed to the release of water and some organics, the others to crystallization processes.

Figure 2 shows the XRD patterns of the samples calcinated at temperatures between 350 ºC and 1000 ºC. It can be observed that the samples treated below 380 ºC are amorphous. The XRD pattern of the sample calcinated at 380 ºC revealed the presence of the anatase phase. The intensity of all diffraction peaks are in accordance with the JCPDS reference (Fig.2) with the exception of their large line width that can be related with small grain size.
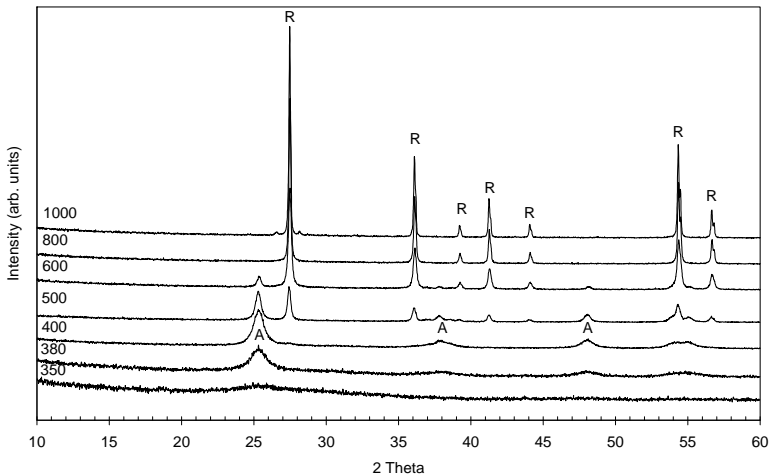

Fig. 2: DRX patterns of the powders treated at temperatures between 350 ºC and 800ºC (A – anatase 01-071-1167; R - rutile 04-005-4859)

The XRD of the samples calcinated at 500 and 600ºC show both anatase and rutile phases. Thus, the 350-380 ºC and 460-480 ºC peaks, observed on the DSC and DTA spectra, should be associated with the formation temperature of the anatase and rutile phases, respectively. The sample calcinated at 800 ºC only presents the XRD pattern of the rutile phase. From the XRD patterns, the crystallite size was calculated (Table1) and the obtained results show that for the both phases (anastase and rutile) the crystallite size increases with the increase of the calcination temperature. The grains size observed in

the SEM micrographs are in accordance with the results obtained from the Scherrer formalism. For the 380 ºC calcinated sample, the SEM micrograph (fig.4a) reveal the existence of particles with a very low size (<<30nm). The increase of the temperature to 400 ºC, lead to a growth of the particles size to a maximum of 30nm. This value, higher than the ~10nm obtained by the Scherrer equation, indicate that aggregation phenomena is occurring and grains are been formed. In the samples calcinated at 500 and 600 ºC, where anatase and rutile phases are both present, the Scherrer equation reveal that the size of the crystallite associated with the anatase phase is higher than the one associated with the rutile phase. Nevertheless, the crystallite size increases with the increase of the calcinated temperature. Crystals with prismatic form, typical of rutile phase, were observed by SEM in the sample calcinated at 800 ºC (fig. 3d). The average size of this crystals, approximately 100nm (fig.3d), is in accordance with the calculated crystallite size (table 1). It should be noticed that the SEM micrographs of the sample calcinated at 1000 ºC (fig.3f) reveal grains well defined and also the grain-boundaries.

Table 1: Crystallite size of all samples calculated by the Scherrer formula at the main phase angle for the anatase and rutile system, grain size obtain from the SEM micrographs analysis, dielectric constant and loss tangent, at room temperature and 1kHz.

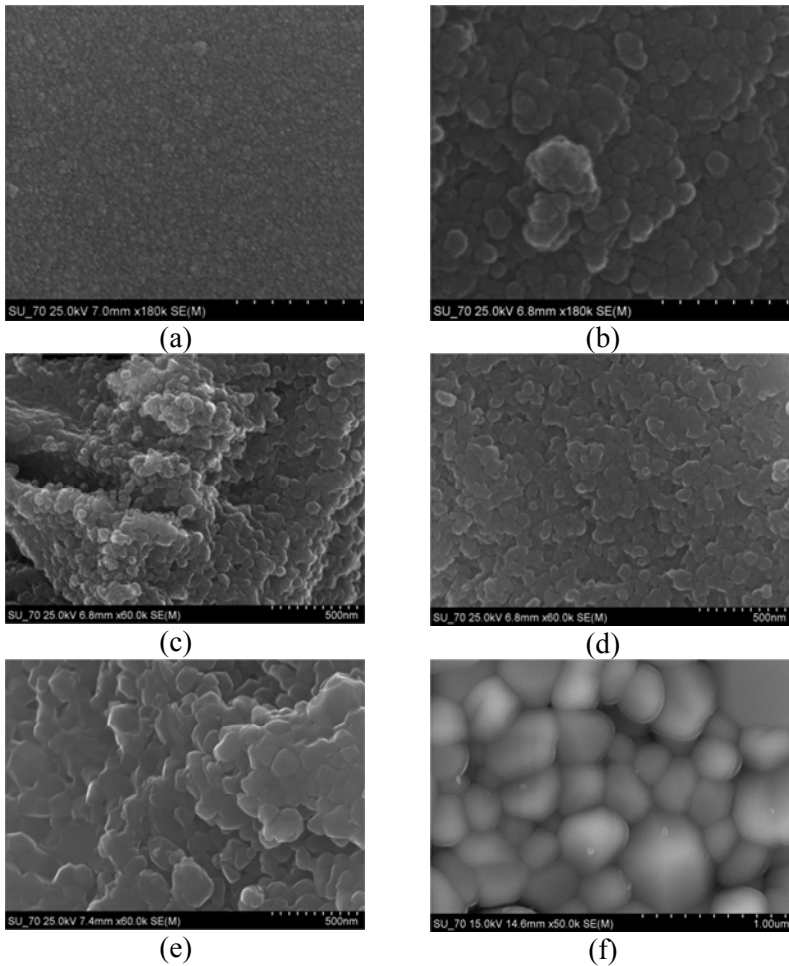| Sample	Crystallite size (nm)		Grain size (nm)	ε	tan δ
	$2\theta \approx 25.4º$	$2\theta \approx 27.4º$			
380	6.89 ± 0.05		--		
400	10.56 ± 0.14		~30	15.87	0.32
500	21.40 ± 0.58	38.90 ± 1.95	~50	16.57	0.17
600	30.08 ± 1.17	46.94 ± 2.80	>50	23.48	0.05
800		102.24 ± 9.15	>100	44.11	0.40
1000		475.73 ± 18.25	>300	195.72	1.92

Fig.3: SEM micrographs of the samples calcinated at: a) 380 ; b) 400 ; c) 500; d) 600, e) 800, f) 1000ºC.

The dielectric results, obtained at room temperature, show that the dielectric constant decreases, in all samples, with the increase of the frequency. At a fixed frequency it can be observed that ε' (table 1, fig.4) increases with the increase of the calcination temperature. This behaviour should be assigned to the increase of the ratio between the anatase and rutile crystal form. It is known that rutile phase has a

dielectric constant higher than the anatase phase [21]. It must be notice that the sample calcinated at 1000 ºC has a large value for the dielectric constant. In agreement with Ye et al. [6] this kind of anomalous dielectric behaviour can be ascribed to interface polarizations.
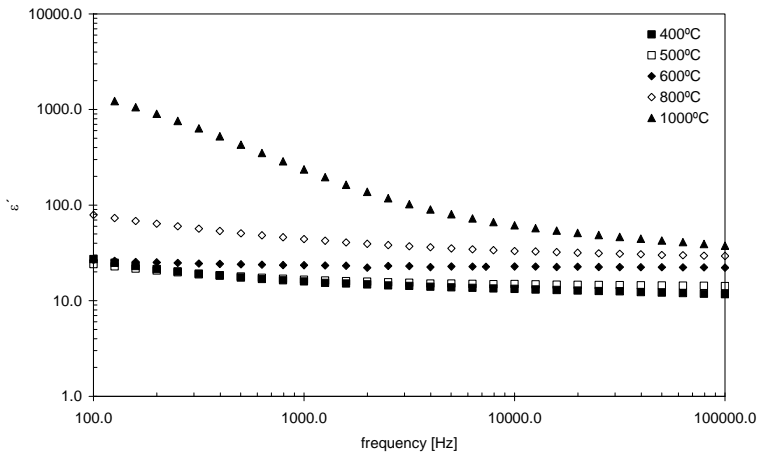

Fig. 4: Dielectric constant (ε') in function of frequency for the samples calcinated between 400 ºC and 1000 ºC, at room temperature.

Figure 5 presents the loss tangent ($\tan \delta = \delta''/\varepsilon'$) of all samples, showing that all samples present high dielectric loss values (>0.02). In this graph ($\tan \delta$ vs frequency) it is observed the existence of a relaxation mechanism, at room temperature and in the frequency window used (100 – 100 kHz), for the sample calcinated at 1000 ºC. In order to analyse the existence (or not) of dielectric relaxation mechanisms, in the other samples, the dielectric data was analysed using several models (impedance, admittance, conductivity [15-17]). Figure 6 shows the results using the modulus formalism being visible the existence, in all samples, a relaxation mechanism.

Figure 7 shows the M´´ behaviour in function of frequency for all samples. It is suggested that the maximum of the M´´ observed on the 400 ºC calcinated sample shifts to lower frequencies with the increase of the calcination temperature. Using the brick layer model to analyse this impedance behaviour, the dipoles from electrodes, grain-

boundaries and bulk should be considered [22]. The use of the modulus formalism is normally chosen in order to minimize the low frequency relaxation mechanism associated with electrode polarization, which is extrinsic to the sample, and maximize the grain-boundary and bulk responses. Hence, it is suggested that the maximum observed in the 400 ºC sample should be related with the dipolar moment formed by the bulk. With the increase of the calcination temperature the volume of the grains increases (Figs.3, table 1), and thus the dielectric relaxation time is expected to decrease. It should be mentioned that in the samples treated at the temperatures of 500 and 600 ºC this peak is not observed in the frequency range (100 Hz- 100 kHz) but the observed trend, at the low frequency range (Fig.7), suggests this hypothesis.
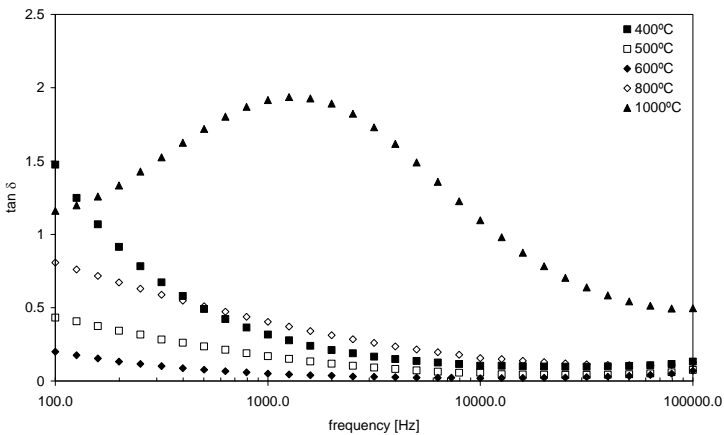

Fig. 5: Loss tangent in function of frequency for the samples calcinated between 400 ºC and 1000 ºC, at room temperature.

The sample calcinated at 800 ºC, which presents only the rutile phase (Fig.3), shows an large increase in the size of the grains when compared to the sample calcinated at 600 ºC. Thus, the M'' maximum due to the bulk is expected to be at frequencies lower than the observed for the sample calcinated at 600 ºC (below 100 Hz). The M'' maximum observed for the 800 and 1000 ºC samples increases

with the rise of the calcination temperature. Knowing that with the increase of the grain size there is a decrease of the surface area, the M'' behaviour can be assigned to the grain-boundary interface polarization [6].
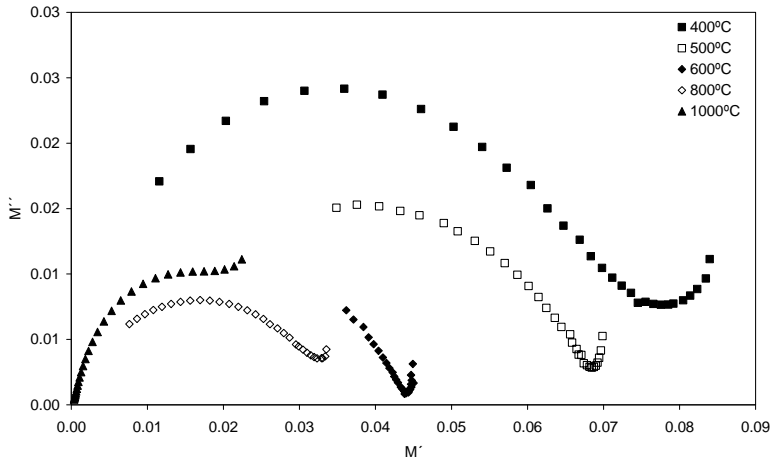

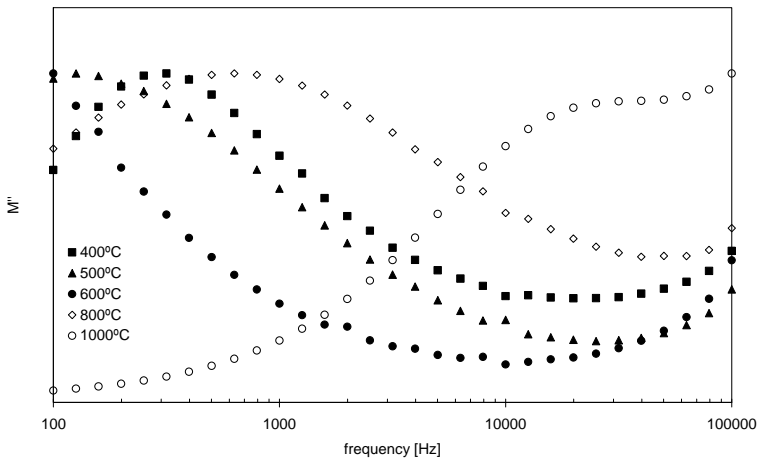Fig. 6: M´ versus M' 'for the samples calcinated between 400 ºC and 1000 ºC.

Fig. 7: M´´, normalized to the maximum value, in function of frequency for the samples calcinated between 400 and 1000 ºC.

4.   Conclusions

The Pechini method was used to prepare TiO_2 nanopowders. Anatase and rutile phases were obtain through a controlled calcination process. Anatase phase is form with calcination temperature above 380 ºC and the rutile phase is also detected in the samples calcinated at temperatures above 500 ºC. For temperatures above 800 ºC, rutile is the only crystal phase present.

The morphology analysis shows that the grain size increases with the increase of the calcination temperature. The sample calcinated at 1000ºC presents different morphology.

The dielectric constant, measured at room temperature, increases with the increase of rutile phase content. The high dielectric constant value observed in the sample calcinated at 1000 ºC was assigned to grain-boundary polarization.

A dielectric relaxation mechanism was observed, in all samples, using the modulus formalism. The relaxation mechanism observed in the samples calcinated at 400, 500 and 600 was assigned to polarization arising from the bulk and the relaxation phenomenon detected in the 800 and 1000 ºC treated sample was associated with grain-boundary polarization.

References

[1]   Cox, Photochemistry **22** (1992) 505
[2]   Kormann, D. W. Bahnemann, M. B. Hoffmann, J. Phys. Chem. **92** (1988) 5196
[3]   O'Regan, M. Gra¨ tzel, Nature **353** (1991) 737
[4]   Mergos JA, Dervos CT, Mater Charact (2009)
[5]   Ulrike Diebold, Surface Science Reports, **48** (2003) 53
[6]   X. Ye, Z. Xiao, D. Lin, S. Huang, Y., Mater. Sci. Eng B**74** (2000) 133
[7]   L. Castañeda, J. C. Alons, A. Ortiz, E. Andrade, J. M. Saniger, J. G. Rañuelos, Mater. Chem. Phys. **77** (2002) 938
[8]   Y. L. Du, Y. Deng, M. S. Zhang, J. Phys. Chem. of Solids **67** (2006) 2405
[9]   S. Rajesh, V.S. Nisa, K.P. Murali, R. Ratheesh, J. Alloys and Comp. (2008)

[10] D. C. Cronomeyer, Phys. Rev B, **87** (1952) 876

[11] X. Chen, S. S. Mao, Chem. Rev. **107** (2007) 289112959

[12] M. P. Pechini, US Patent no. **3** (1967) 330

[13] C. C. Silva, M. P. F. Graça, M. A. Valente and A. S. B. Sombra, J. Mat. Sci. **42** (2007) 3851

[14] M. P. F. Graça, M. A. Valente, M. G. Ferreira da Silva, J. Mat. Sci. **41** (2006) 1137

[15] J. R. Macdonald, "*Impedance spectroscopy*", John Wiley & Sons, New York (1987)

[16] A. K. Jonscher, "*Dielectric relaxation in solids*", Chelsea Dielectrics Press, London (1983)

[17] B. V. R. Chowdari, K. Radhakrishnan, J. Non-Cryst. Solids, **110** (1989) 101

[18] P. B. Macedo, C.T. Moynihan, R. Bose, Phys. Chem. Glasses, **13** (1972) 171

[19] J. C. C. Abrantes, J. A Labrincha, J. R. Frade, Mat. Res. Bull., **35** (2000) 727

[20] Kia L. NGai, Ronald W. Rendell in: *Handbook of conducting polymers*, vol II, Marcel Dekker, N.Y. (1986)

[21] G. F. Dionne, J. F. Fitzgerald, R. C. Aucoin, J. Appl. Physics **47** (1976) 1708

[22] D. Eder, R. Kramer, J. Phys. Chem B **108** (2004) 14823